School of Mathematics, Computer Science and Engineering

"Optimised Radial Turbine Design D1.8"

By

Mahmoud Khader

Approved by:

Professor Abdulnaser I Sayma

London

October 2014

SUMMARY:

This report presents the design of a radial turbine to match the requirements of a 5 kWe solar powered micro gas turbine. This report is part of City University's responsibility to design an optimised solar powered microgas turbine for the OMSoP (Optimised Microturbine Solar Power system) project. A meanline design has been used to obtain the main geometry parameters for the turbine parts. The results were used to generate the three-dimensional geometry of the parts. The geometry was then tested using Computational Fluid Dynamics (CFD), where some modifications on the preliminary design were introduced to satisfy the design requirements. After reaching an aerodynamically mature design, the geometry was tested using Finite Element Analysis (FEA) tools. This step included modifying the geometry to ensure the structural integrity during operation. The turbine design aimed to obtain a high efficiency to meet the target requirements of the Concentrated Solar Power (CSP) system.

The turbine's design point rotational speed is 130,000 rpm, stagnation inlet temperature and pressure are 800 C°, 2.92 bar respectively and mass flow rate is 0.08 kg/s. The turbine rotor has 13 blades with inlet and exit diameters 73.4mm and 42.2 mm. 15 uncambered nozzle guide vanes have been designed as they are easy to manufacture and provide a good performance. The efficiency of the designed turbine has reached 83.8% at the design point. Computations were performed to ensure that the turbine is able to run efficiently and withstand temperatures if the receiver was able to reach turbine inlet temperature of 900 ^{o}C. The presented turbine design is specifically for the demonstration plant, but the developed methodology will be used to design a turbine for the final optimised system.

Table of Contents

NOMENCLATURE:

A	Area
b	Rotor inlet blade height
C	Flow absolute velocity, Chord length
C_p	Specific heat at constant pressure for air
D	Diameter
h_v	Nozzle guide vane height
I_g	Interspace geometry parameter
$\dot{m}$	Mass flow rate
N_s	Specific speed
N_b	Number of rotor blades
N_{gv}	Number of nozzle guide vanes
P	Pressure
PR	Pressure ratio
$\dot{Q}$	Rotor outlet volume flow rate
R	Universal gas constant
R	Radius
S_v	Guide vanes pitch
T	Temperature
t	Thickness
U	Blade speed
W	Flow relative velocity
Z	Rotor axial length
ρ	Density

Greek Letters

Δh_o	Enthalpy change across turbine rotor
ζ	Rotor meridional velocity ratio
β	Relative flow angle
α	Absolute flow angle
ψ	Blade loading coefficient
ω	Rotational speed
ϕ	Flow coefficient
η	Efficiency
ν	Velocity ratio
γ	Specific heat ratio

Subscripts

1	Turbine inlet
2	Nozzle guide vanes outlet

3	Rotor inlet
4	Rotor Outlet
5	Compressor inlet
6	Compressor discharge
amb	Ambient
comp	Compressor
el	Electrical
gen	High speed generator
h	hub
le	Leading edge
m	Meridional component
max	Maximum
mech	Mechanical
o	Total thermodynamic condition
r	Recuperator
st	Stator
t	Tip
te	Trailing edge
turb	Turbine
ts	Total to static
θ	Tangential component, Guide vane angle
ν	Nozzle guide vane

Abbreviations

CFD	Computational Fluid Dynamics
HSG	High Speed Generator
FEA	Finite Element Analysis
ISA	International Standard Atmosphere
KTH	Royal institute of technology (OMSoP partner)

INTRODUCTION:

A Turbine for a 5 kWe microgas turbine has to be designed as a part of a project funded by the European Commission called OMSoP (Optimised Microturbine Solar Power system). The project is made as an approach to reduce the global CO_2 emissions by providing technical solutions for the use of concentrated solar power systems coupled to microgas turbine. City University is the coordinator of the project and it is responsible for designing an optimised Micro-Gas turbine.

Cycle analysis calculations for the gas turbine were carried out before starting the design process. Using these calculations, the cycle parameters corresponding to the best achievable efficiency within the allowable working limits were evaluated. This optimum efficiency point is regarded as the design point. The results for the design point give the data needed to start up the turbine design process.

The turbine design process starts by using the specifications obtained from the cycle analysis in a preliminary design tool where one-dimensional calculations are used to generate the overall dimensions required to construct the three-dimensional geometry for the turbine parts. The second stage then is to generate the geometry of three-dimensional geometry. The third is the verification of the aerodynamic performance using Computational Fluid Dynamics (CFD). According to the CFD results improvements to the design may be required. Hence the design process may require iterations until the specified design requirements are satisfied. Finally, the turbine materials are chosen and Finite Element Analysis (FEA) is performed to check its structural integrity of the turbine. If the FEA indicates a potential failure under operating loads, modifications to the geometry such as removing material between rotor blades (scalloping) or introducing larger fillet radii should be done.

This report is devoted to detailing the design process and the resulting design, starting from the basic performance characteristics, through to obtaining a design ready for manufacturing and testing.

2- THE DESIGN PROCESS:

The radial turbine is a work-producing device that consists of moving and stationary parts. Figure 1 shows a schematic diagram for a radial turbine and its components. The turbine has a stationary component (stator) and rotating component. The stationary component is compromised of an annular ring called the volute and set of nozzle guide vanes. The rotating part which is the heart of the turbine called the rotor.

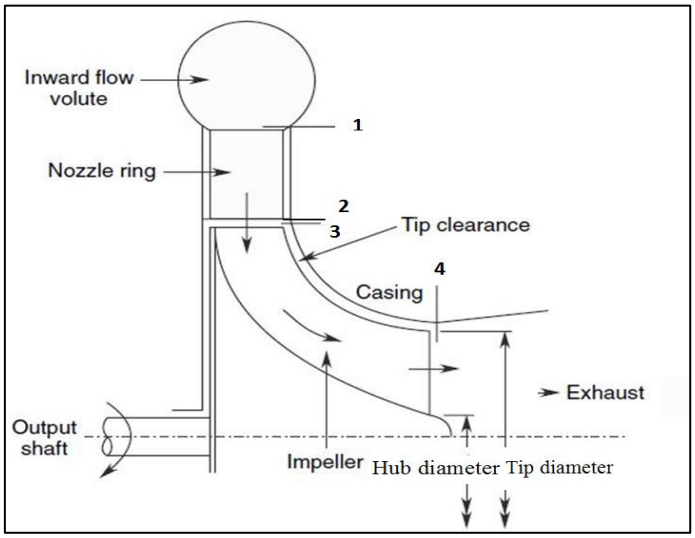

Figure 1: Radial turbine components.

The design process used in this work is comprised of three steps: the meanline (one-dimensional) design, geometry generation and performance and structural analysis using CFD and FEA tools. Turbine design is an iterative process, where iterations are needed between CFD results and preliminary design results and between the FEA results and geometry details. Figure 2 summarises the design process that is used in this work.This section briefly describes the design steps and provides details for the meanline design process, CFD and FEA setup are given in the following sub sections.

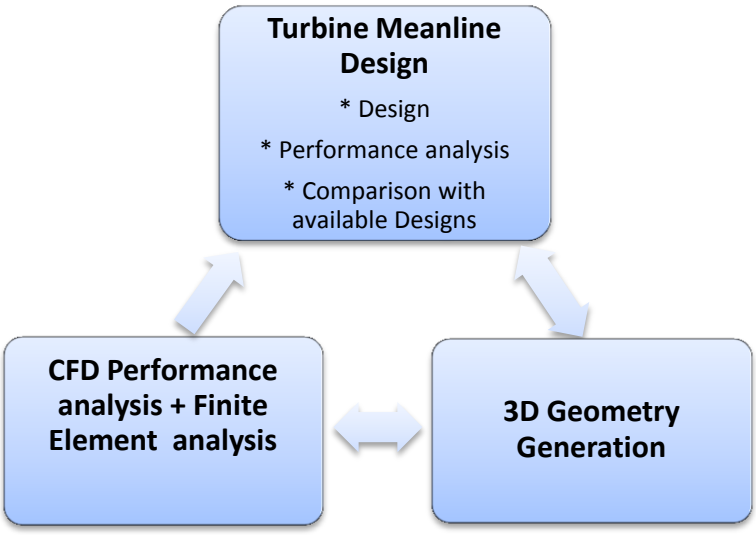

Figure 2: Turbine Design Process diagram.

The thermodynamic properties of the working fluid entering the turbine and the expected performance of the designed machine are obtained from the cycle analysis for the gas turbine taking into account that the turbine is connected to the solar receiver. Based on these parameters and the performance parameters available in the literature for; the appropriate thermodynamic and fluid dynamic conservation principles are applied within the preliminary design process in order to obtain the following:

- The main geometric parameters of components such as the mean radii, blade height and blade angles at inlet and outlet of the rotor wheel.
- Thermodynamic quantities at the inlet and outlet of each component.
- Flow velocity at the defined stations.

The next step is to generate the three-dimensional geometry. Based on the parameters gained from the meanline design the 3D-geometry can be generated. For the turbine rotor geometry the commercial software ANSYS Bladegen was used. In Bladegen the inputs are the radii of the turbine wheel at inlet and exit, the blade angles and the blade thicknesses. Blade thicknesses are given an initial guess which are then modified according to stress analysis results. The geometries of the remaining parts were built using SolidWorks.

The next step is to check performance by analysing the flow using CFD. Grids were generated using ANSYS Turbo-Grid and ANSYS CFX was used to obtain the steady state flow solutions. The following boundary conditions were used:

- Total temperature, total pressure and flow angles at inlet.
- Rotational velocity for the rotating part.
- Static pressure at rotor exit.

The outcomes from the CFD were:

- Performance predictions in the form of pressure drop and isentropic efficiency.
- Distribution of flow quantities throughout the turbine.

CFD results indicated some modifications on the geometry of the rotor blades angles and blade numbers are required. Also the nozzle guide vanes angles, number and the space between the guide vanes and the rotor have been modified. The design process was iterated until an aerodynamically satisfactory design has been reached.

The final step after setting the parts design is to perform a steady state stress analysis to check the design rigidity under the operating loads. For this purpose the commercial software ANSYS Mechanical was used to perform the FEA analysis on the turbine rotor as it is the most critical part and exposed to the highest loads. The rotor geometry was modified according to the FEA results, by changing the blades thickness, cutting material from the back face of the rotor, introducing fillets at contact edges between the blades and the hub of the rotor and by cutting material between the rotor blades near the leading edge, in a process

called scalloping. Scalloping is used to reduce the mass and the inertia of the turbine rotor and also to reduce the stresses at the point of contact between the back face of the rotor and the rotating shaft.

2.1- GAS TURBINE CYCLE ANALYSIS:

The overall specifications of the micro-gas turbine requires for the demonstration plant have been decided by the project consortium based on overall system considerations. Following this step, Cycle analysis and optimisation was performed at City University London to determine cycle parameters required for the design of the micro-gas turbine components. This subsection outlines the main outcomes of the cycle analysis pertinent to the design of the turbine. The micro-gas turbine is based on a simple recuperated cycle as shown in Figure 3, where the receiver replaces the combustion chamber. A design point Turbine Inlet Temperature (TIT) of 800^{o}C was specified by KTH as the maximum achievable for the demonstration plant. However, higher temperatures will be targeted for the final optimised system.

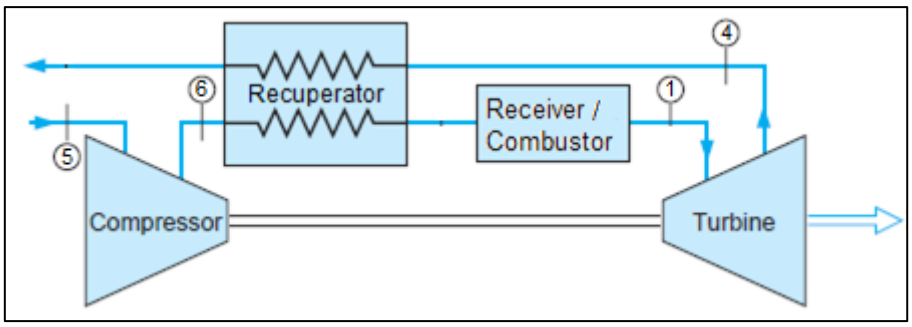

Figure 3: Schematic diagram of the micro-gas turbine cycle.

Table 1 shows the component parameters specified for the cycle analysis based on estimated achievable component efficiencies.

Table 1: Micro-gas turbine components parameters

Parameter	value
Ambient temperature	288.15K
Ambient pressure	1.01325bar
Compressor efficiency	74%
Turbine efficiency	80%
Recuperator effectiveness	85%
Receiver efficiency	80%
Electrical efficiency	90%

Using these parameters, cycle analysis was performed for a range of compressor pressure ratios (PRc), (TIT) and turbine exit temperature (TET). Estimated component pressure losses were also taken into consideration. Figure 4 shows a summary of the cycle analysis results which allowed for specifications required for the turbine design.

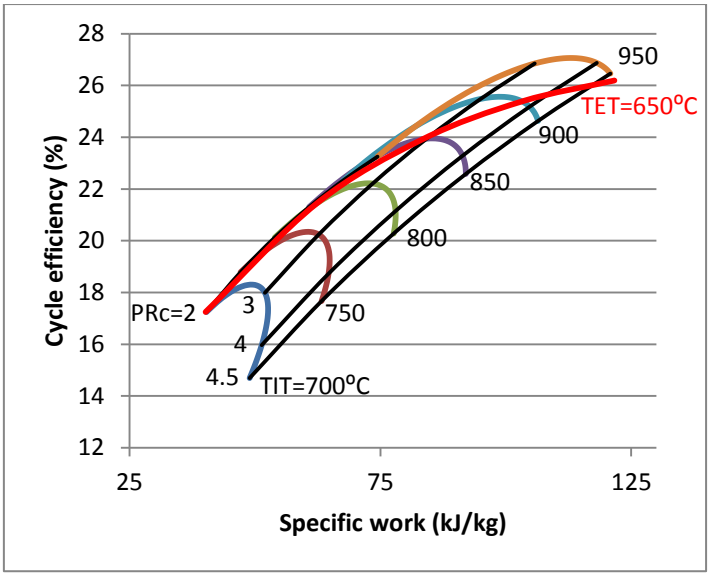

Figure 4: Performance diagram for different cycle parameters

It can be seen that higher TIT leads to higher efficiency and specific work which are desirable in general, but turbine inlet temperature is limited by materials considerations and maximum temperature attainable by the receiver as mentioned above. A constant TET 650^{o}C line is also shown in figure 4 as this temperature is the maximum allowed for a stainless steel recuperator. The TET line shows that for turbine inlet temperatures higher than 800 ^{0}C, the recuperator will be overheated at low pressure ratios. This is the case when running the engine at low speeds. At TIT of 800^{o}C, maximum cycle efficiency occurs at pressure ratio of three. Using the selected pressure ratio and turbine inlet temperature, the cycle analysis results which are related to the turbine are summarised in table 2. A rotational speed of 130,000 rpm was selected to achieve the highest compressor and turbine efficiency at their respective specific speeds.

Table 2: Cycle analysis results

Parameter	Value
Turbine inlet total pressure (bar)	2.919
Turbine inlet total temperature (K)	1073
Turbine mass flow rate (kg/s)	0.08
Power generated by turbine (kW)	18.02

2.2- MEANLINE DESIGN:

A mean line or one-dimensional design approach is the application of basic equations and empirical relations to calculate the overall design parameters. Mean line design is a good approach to get the first estimate for the radial turbomachine design and analysis as it is a fast method and needs a small amount of information regarding the turbomachine geometry. Also, a number of design options can be checked before moving to advanced stages of system design including three dimensional geometry construction and computational analysis software.

To start the mean line design calculation; two sets of data need to be provided to the design program. The first is taken from the gas turbine cycle analysis; the parameters needed from the cycle analysis are:

- Turbine inlet total temperature.
- Turbine inlet total pressure.
- Mass flow rate.
- Required output shaft power.

The second set comprises empirical relations that are combination of performance and dimensionless ratios available. In the next sub sections those sets of data would be discussed in more details.

Based on the data gained from cycle analysis and literature, the velocity triangle (figure 5), stagnation and static temperature and pressure and rotor inlet diameter and blade height can be calculated. The majority of the internal rotor losses are functions of the fluid velocity, and to improve the efficiency of the rotor the velocity at rotor inlet should be reduced as much as possible to reduce the incidence loss occurring at the rotor inlet. The loading coefficient would be used to minimise the fluid velocity at the rotor inlet.

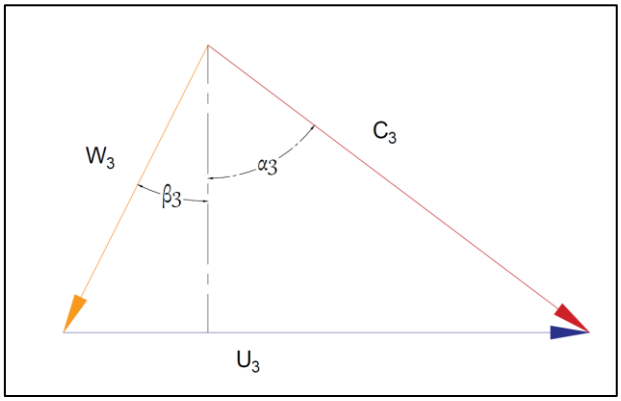

Figure 5: Velocity triangle at rotor inlet.

The velocity triangle components at the rotor inlet are related by the following equation:

$$C_3{}^2 + U_3{}^2 - 2C_3U_3 \sin\alpha_3 - W_3{}^2 = 0$$

And from the definition of the loading coefficient $\left(\psi = \frac{C_3 \sin\alpha_3}{U_3}\right)$ the previous equation become:

$$\psi^2 - 2\psi \sin^2\alpha_3 + \sin^2\alpha_3 \left[1 - \left(\frac{W_3}{U_3}\right)^2\right] = 0$$

The solution for this equation is

$$\psi = \sin^2\alpha_3 \pm \sin\alpha_3 \sqrt{\left(\frac{W_3}{U_3}\right)^2 - \cos^2\alpha_3}$$

For ψ to be real the condition would be:

$$\left(\frac{W_3}{U_3}\right)^2 \geq \cos^2\alpha_3$$

The minimum value of $\frac{w_3}{u_3}$ occurs when

$$\frac{W_3}{U_3} = \cos\alpha_3$$

The loading coefficient and the rotor inlet calculations are iterated until the condition above are satisfied. After finishing that loop the rotor exit velocity triangle, stagnation and static temperature and pressure and rotor exit diameter and blade height can be calculated.

For the guide vanes design; a combination of the geometrical parameters selected from the literature and rotor design were used to calculate the dimension of the guide vanes. Based on the guide vanes inlet diameter and width the geometry of the volute were calculated.

2.2.1- PERFORMANCE PARAMETERS:

Table 3 contains the design parameters available in literature for radial turbines design. This section outlines the reasoning behind the choice shown in table 3.

Table 3: Design parameters.

Parameter	Value
Stage Loading Coefficient (ψ)	0.8
Ratio of axial length to rotor inlet radius $\left(\frac{Z}{r_{t3}}\right)$	0.7
Exit flow coefficient (ϕ)	0.25
Rotor meridional velocity ratio ($\zeta = \frac{C_{m3}}{C_{m4}}$)	1
Exit hub to inlet tip radius ratio $\left(\frac{r_{4h}}{r_3}\right)$	0.3
Vane chord to rotor inlet diameter $\left(\frac{C_v}{D_3}\right)$	0.3
Vane chord to vane pitch (solidity) $\left(\frac{C_v}{S_v}\right)$	1.2
Thickness of vane leading edge to vane chord $\left(\frac{tv_{le}}{C_v}\right)$	0.285
thickness of vane trailing edge to vane height $\left(\frac{tv_{te}}{h_v}\right)$	0.12
Inter-space geometry parameter (I_g)	2

Starting with the blade loading coefficient, as shown in figure 6 the maximum efficiency of the loading coefficient ranges between (0.8 - 0.1). In the designed program starting with a value of 0.8 an iterative process is followed until reaching a value where the incidence loss would is minimised. Another important parameter is the exit flow coefficient which is related to the loading coefficient as shown in figure 6. It is clear that the best efficiency range is (0.2-0.3), a value of 0.25 was chosen as it corresponds to the highest efficiency.

The ratio of axial length to rotor inlet radius$\left(\frac{Z}{r_{t3}}\right)$was chosen to be 0.7 as recommended by Whitefield and Baines 1990 as this geometric value depends on past experience and there are no correlations to determine it. The value of exit hub to inlet tip radius ratio$\left(\frac{r_{4h}}{r_3}\right)$was chosen to be 0.3 according to Baines 2003 and Jacob et al 2012. The rotor meridional velocity ratio normally has a value near 1.0 as suggested by Baines 2003.

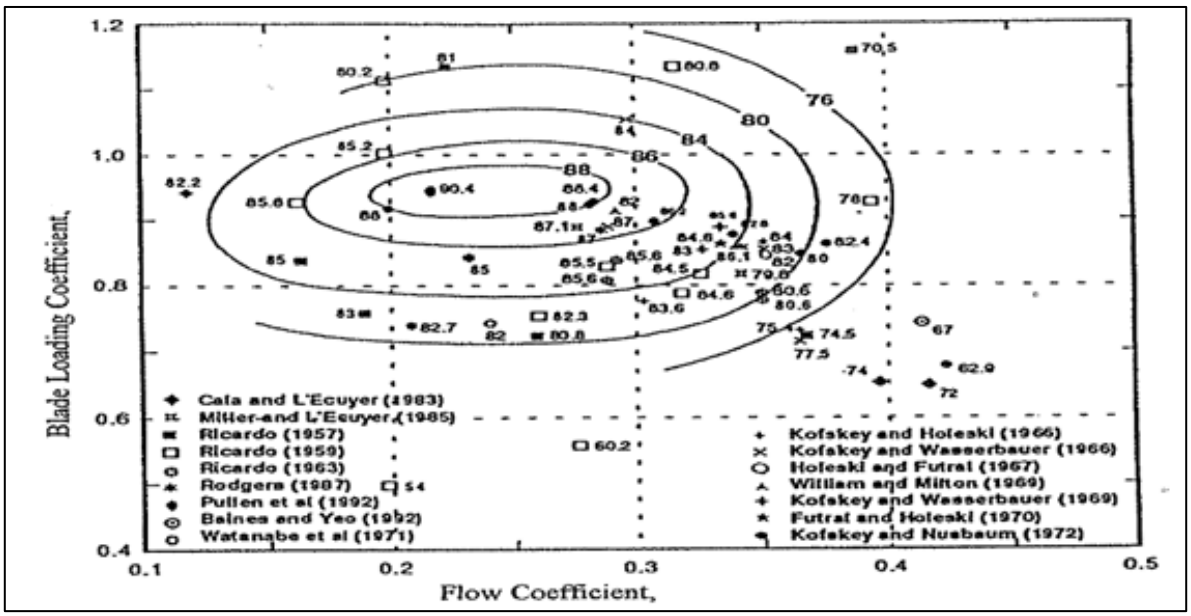

Figure 6: Correlation of attainable radial turbine efficiency Baines (2003).

A stator loss coefficient of 0.08 was assumed, which is feasible for the turbine stator. The turbine total to static efficiency assumed to be 90%; this means that this design is aiming for higher efficiency than the target.

For designing the nozzle guide vanes design, the vane chord to rotor inlet diameter $\left(\frac{C_v}{D_3}\right)$ was selected to be 0.3 as suggested by Heitt and Johnston 1964. The values of Vane chord to vane pitch (solidity) $\left(\frac{C_v}{S_v}\right)$, Thickness of vane leading edge to vane chord $\left(\frac{tv_{le}}{C_v}\right)$ and thickness of vane trailing edge to vane height $\left(\frac{tv_{te}}{h_v}\right)$ where given values of 1.2, 0.285 and 0.12 respectively following the recommendations of Aungier 2006. The interspace geometry value $\left(\frac{r_{v2}-r_3}{h_v \times \sin \alpha v}\right)$ recommended by Watanabe et al (1971) for minimum losses was suggested to be two.

3- DESIGN RESULTS:

This section contains the preliminary design results, the CFD results and the FEA analysis results for the designed turbine.

3.1 PRELIMINARY DESIGN RESULTS:

Table 4 shows the design results obtained from the mean line design process.

Table 4: Meanline design results.

Parameter	Design Results	Units
Rotor total inlet temperature (T_{o3})	1073	kelvin
Rotor static inlet temperature (T_3)	978	kelvin
Rotor total exit temperature (T_{o4})	878	kelvin
Rotor static exit temperature (T_4)	871	kelvin
Rotor total inlet pressure (P_{o3})	2.92	bar
Rotor static inlet pressure (P_3)	1.948	bar
Rotor total exit pressure (P_{o4})	1.216	bar
Rotor static exit pressure (P_4)	1.179	bar
Rotor inlet radius (r_{t3})	0.0367	m
Rotor Exit radius (r_{4t})	0.0211	m
Exit hub radius (r_{4h})	0.0011	m
Rotor axial length (Z)	0.0257	m
Rotor inlet height (b_3)	0.004	m
Rotor tip velocity at rotor inlet (U_3)	499	m/s
Flow relative velocity at rotor inlet (W_3)	135	m/s
Absolut flow velocity at rotor inlet (C_3)	467	m/s
Rotor tip velocity at rotor exit (U_{4rms})	229	m/s
Flow relative velocity at rotor exit (W_{4rms})	261	m/s
Absolut flow velocity at rotor exit (C_{4rms})	125	m/s
Specific speed (N_s)	0.5	-
Absolut flow angel at rotor inlet (α_3)	74	Degree
Absolut flow angel at rotor inlet (α_4)	0	Degree
Relative flow angel at rotor inlet (β_3)	-21.8	Degree
Absolut flow angel at rotor inlet(β_{4rms})	-61	Degree
Absolut flow angel at vane exit(α_2)	76	Degree
Nozzle vanes Trailing edge radius ($\frac{tv_{te}}{2}$)	0.00315	m
Nozzle vanes leading edge radius ($\frac{tv_{le}}{2}$)	0.000245	m
Nozzle vanes height (h_v)	0.00416	m
Number of nozzle guide vanes (N_{gv})	14	-

A volute with a circular cross section methodology was also implemented in the program. The program calculates the area and the centreline coordinate for each circular cross section

of the volute at different angle starting from 0° to 360°. The volute dimension can be found in table 8 in the Appendix.

The turbine rotor blades were generated using ANSYS baldegen, with the dimensions and the angles were taken from the preliminary design results. Nozzle guide vanes geometry was generated in SolidWorks. Volute geometry was generated using SolidWorks based on the preliminary design data (see table 8). Figure 7 shows the designed volute geometry. Figure 8 shows the distribution of the guide vanes around the rotor and the dimensions of a single vane. From figure 8 it can be noticed that there is 15 guide vane, where the preliminary design results gives 14 blades; this modification has been done so that the turbine can deliver that mass flow rate value similar to that value given by the cycle analysis. The vanes angle (θ) has been iterated to according the CFD results to get the proper incidence angle, where, no separation of the flow was detected.

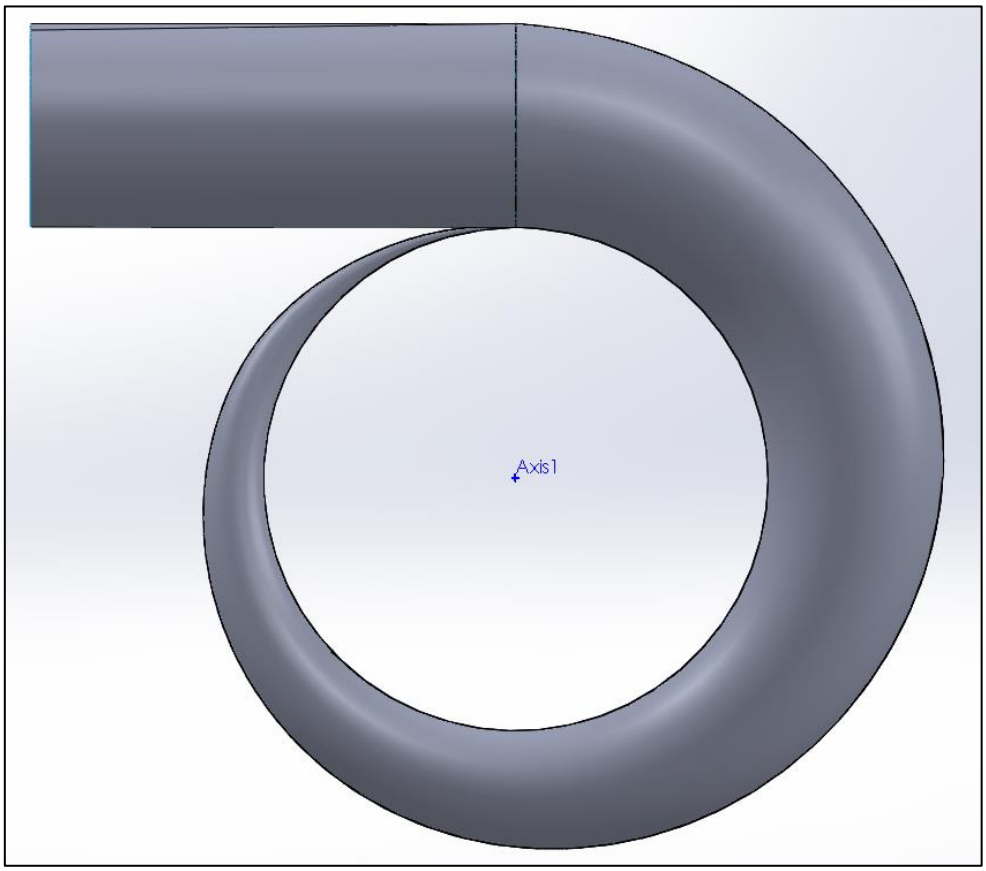

Figure 7: Turbine volute geometry.

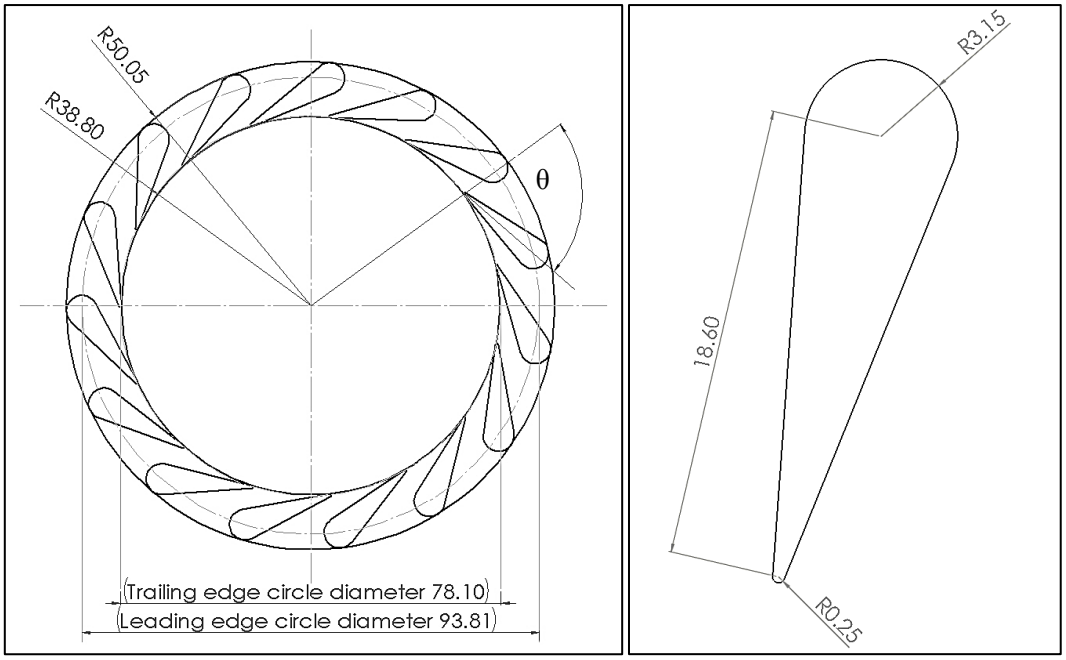

Figure 8: Nozzle guide vanes Geometry.

Figure 9 shows a front and right side view of the rotor. The rotor was scalloped and some material was removed from the rotor back face according to the FEA results, the modifications on the turbine geometry would be discussed in section 3.3.

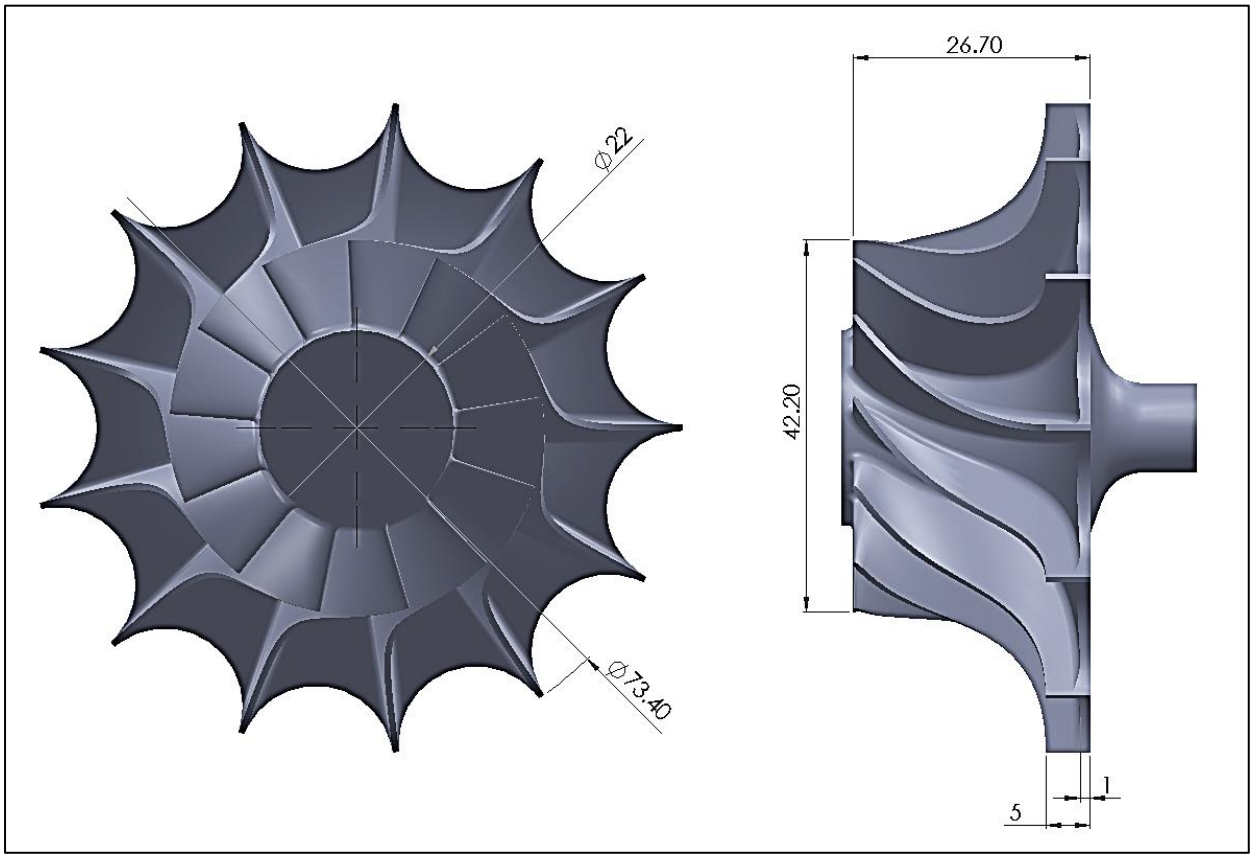

Figure 9: front and Right-side view for the designed rotor wheel (units are in mm).

Figures 10 and 11 show the velocity triangles at rotor inlet and exit respectively. These figures compare the CFD results with those obtained from the one-dimensional design process. The velocity triangles in figure 11 are defined at Root Mean Square (RMS) radius of the rotor outlet.

Based on the CFD results, the number of nozzle guide vanes was increased to 15 to achieve the required mass flow rate. The incidence angle at the rotor inlet was reduced to prevent flow separation at the suction side of the rotor blades. The difference between mean-line design and CFD results shown in figure 10, results from these modifications and the inherent assumptions of the mean line design process.

At the rotor exit (figure11), larger difference can be observed between the CFD results and the meanline results which are related to the assumption made in the preliminary design method.

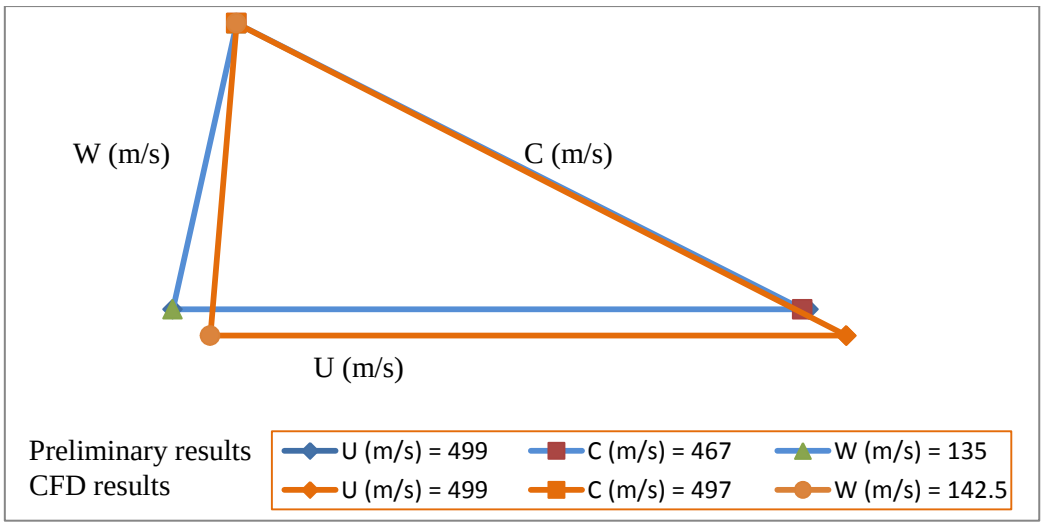

Figure 10: velocity triangle at rotor inlet resulted from preliminary design and CFD results.

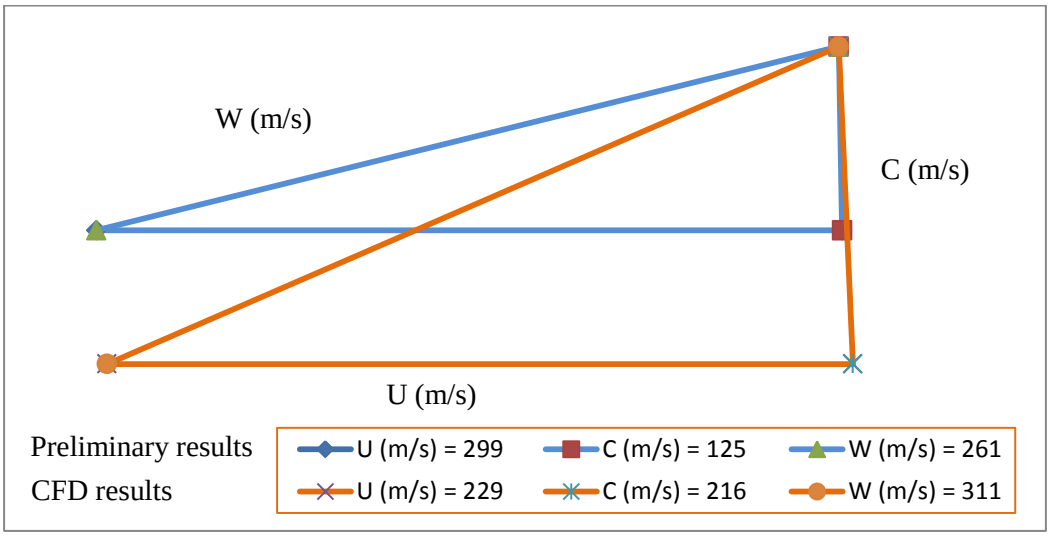

Figure 11: velocity triangle at rotor outlet resulted from preliminary design and CFD results defined at RMS radius.

3.2 CFD RESULTS:

As mentioned previously the CFD has been done using ANSYS. The computational domain for the radial turbine consists of one stator vane and one rotor blade. Structured meshes were generated using ANSYS TurboGrid. To ensure mesh independence, a grid independence study has been performed. Three different parameters (mass flow rate, turbine total to total efficiency and) were calculated from CFD. Six grids of increasing refinement have been used to calculate theses parameters, starting with a coarse grid of 20000 elements and ending with a grid of 1366922 elements. Results shows that increasing number of mesh elements will not affect the results starting from 600000 elements distributed between the rotor and stator domains, hence the stator passage required ~ 250,000 elements and the rotor passage required ~ 350,000 elements. The total number of elements was 621230 elements.

Figure 12 shows the computational domain at ANSYS CFX, the figure shows the surface grid for the computational domain. Coarser mesh is presented for better visualisation.

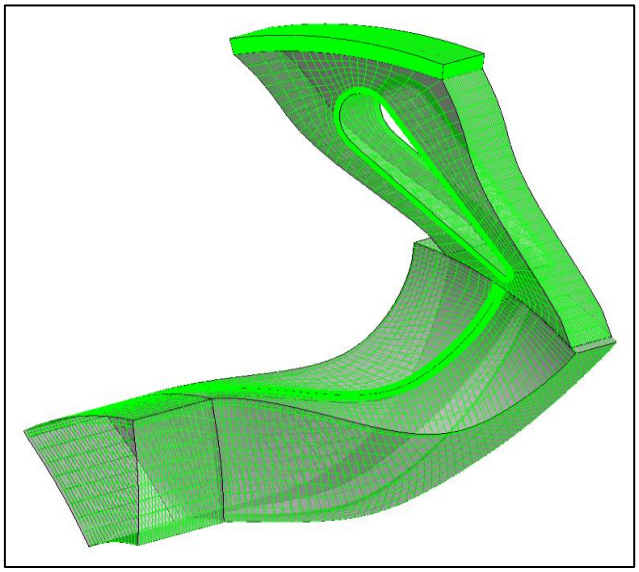

Figure 12: Surface grid for the computational domain.

The numerical calculations were performed using ANSYS CFX. The boundary conditions used for the design are listed in table 5:

Table 5: boundary conditions used in CFD calculations.

Total temperature at domain inlet (Kelvin)	1073
Total pressure at domain inlet (bar)	2.919
Flow angle at domain inlet (degree)	0 (Radial direction)
Rotational speed (rpm)	130,000
Exit static pressure (bar)	1.033

The exit static pressure was set a value 1.033 which equals to the ambient pressure plus the pressure drop in the recuperator.

The rotational periodic boundary condition is imposed on the periodic boundaries. And the non-slip and adiabatic conditions were applied on all solid walls. The connection option of the stator and rotor domains is 'stage' which performs circumferential averaging of the fluxes through bands on the stator and rotor domain interface. A counter-rotating wall condition is specified for shroud, where a tip clearance of 4% of the blade local span was used. The low Reynolds number shear stress transport (SST) k–ω turbulence model, which predicts any flow separation with reasonable accuracy, was employed in the calculations.

Both design point and off-design conditions were simulated to obtain full performance maps. Testing the performance of the designed turbine was performed using CFD. Also, one-dimensional loss models available in literature were used to account for the losses that haven't been considered in the CFD calculations, such as volute and windage losses and the loss due scalloping the turbine rotor. This procedure gives more accurate results to predict the performance of the turbine than using one-dimensional correlations only.

Figure 13 shows the performance map for the turbine at three different rotational speeds, where, the red circle represents the design point. At the design point the mass flow rate of the turbine is 0.0818 and the total to static pressure ratio is 2.827, where the shaft power output from the turbine equals 18.162 kW.

Figure 14 shows the efficiency versus pressure ratio for the same two speeds, where the design point is marked by a red circle. The turbine efficiency gained when operating the turbine at the design point is 83.8%. Also it can be noticed that running the turbine with the same inlet conditions as the design point but with a higher rotational speed (140 krpm) will increase the turbine efficiency to 84.5%, meanwhile, reducing the rotational speed to (115 krpm) will reduce the turbine efficiency to 80.9%. For low expansion ratios (less than 2.2) it can be seen that for the design rotational speed (130 krpm) the efficiency drops significantly, while it increases for lower rotational speed (115 krpm).

Table 6 gives the overall performance for the designed machine when running at the design point as indicated from the CFD results.

Table 6: overall Performance Results Table

Inlet Mass Flow Rate (kg/s)	0.0819
Inlet Volume Flow Rate (m^3/s)	0.0861
Total to static Pressure Ratio	2.827
Total-to-Total Isentropic Efficiency %	83.8
Rotation Speed (rpm)	130,000
Shaft Power (watt)	18162
Nozzle loss coefficient	.08

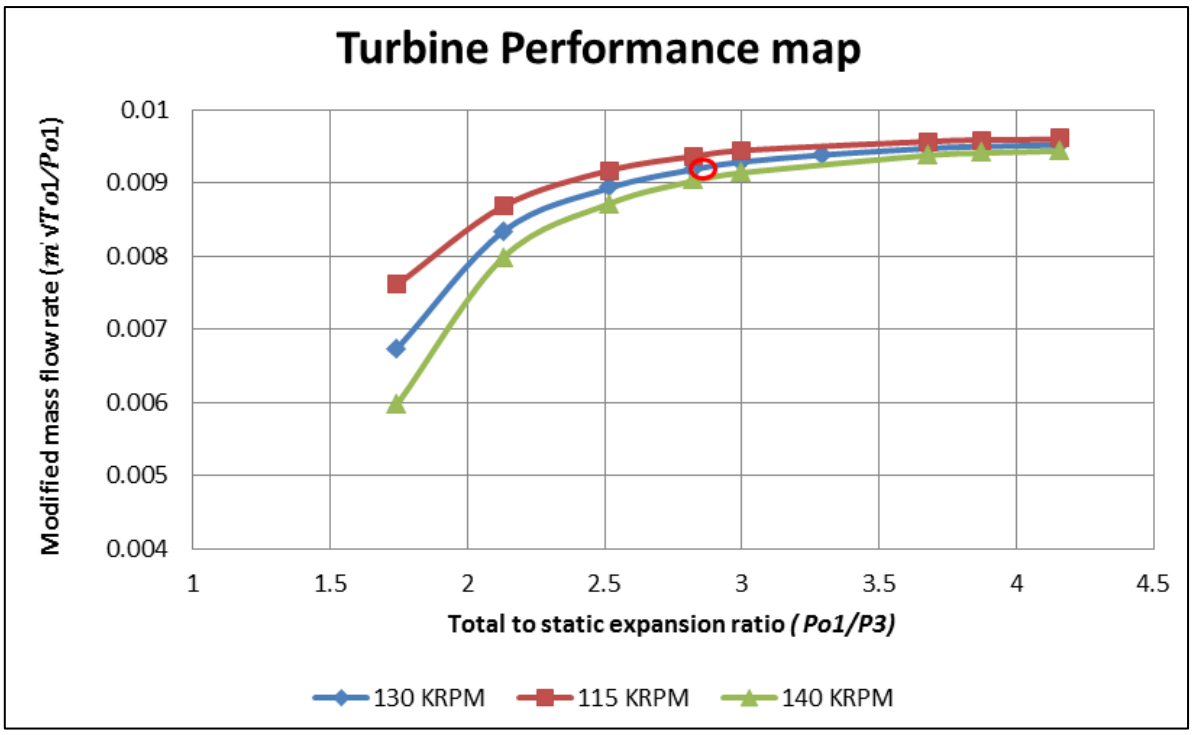

Figure 13: Turbine performance map

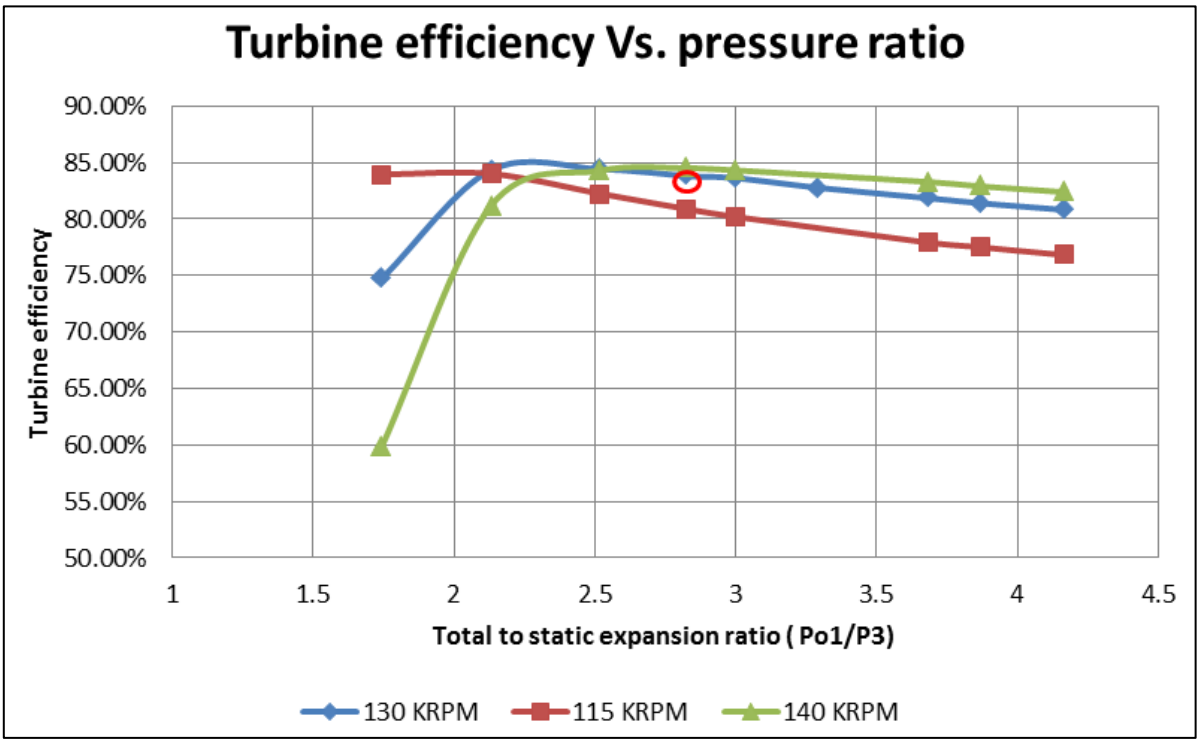

Figure 14: Turbine efficiency versus pressure ratio.

Figure 15 shows the relative velocity contours and vectors at 50% of span of the turbine vanes and rotor. No separation was detected at the design point; the guide vanes angle and number of rotor blades were iterated a number of times to avoid flow separation which is a major source of loss.

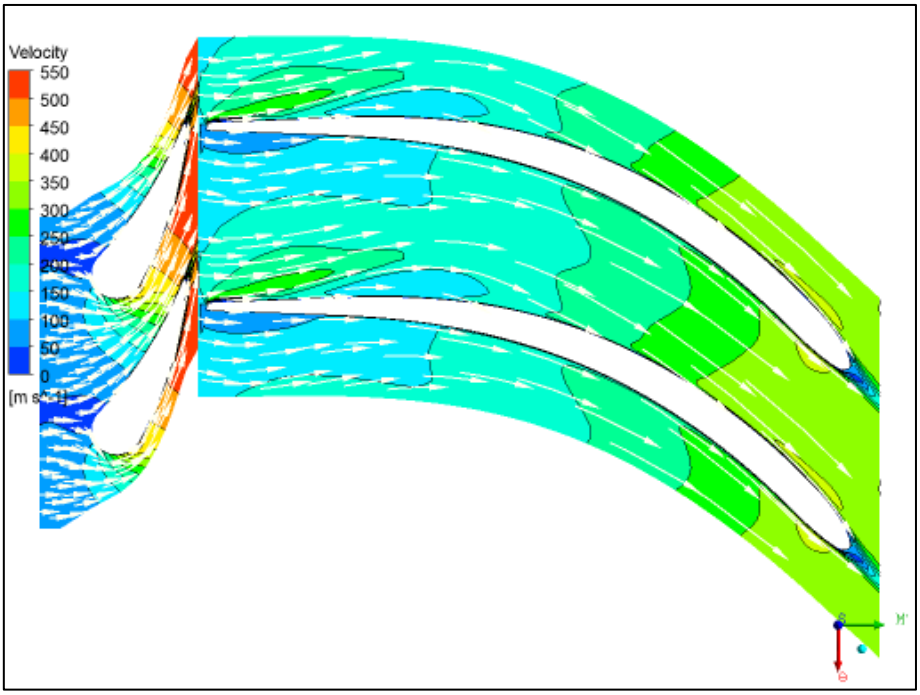

Figure 15: Contours of relative velocity at 50% span

Figure 16 shows the relative Mach number contours at 50% of span for the turbine vanes and rotor, from this figure no choking is expected to happen along the flow passage.

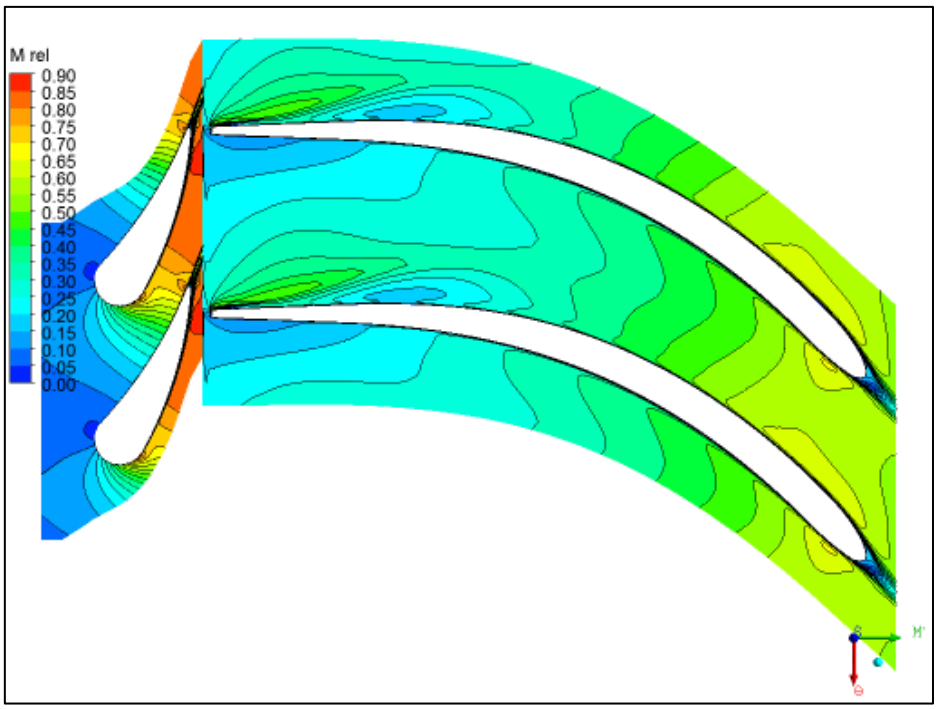

Figure 16: Contours of relative Mach number at 50% span

The blade loading was checked to make sure that the flow is not forced to reverse direction near the trailing edge. Figure 17 shows the blade loading through the rotor passage at 50 % span. The red circle is the region where the flow is usually forced to reverse direction because the pressure at suction surface becomes larger than that on the pressure surface. This pressure reversal causes losses in the turbine, so in this design this reversal in the pressure has been avoided.

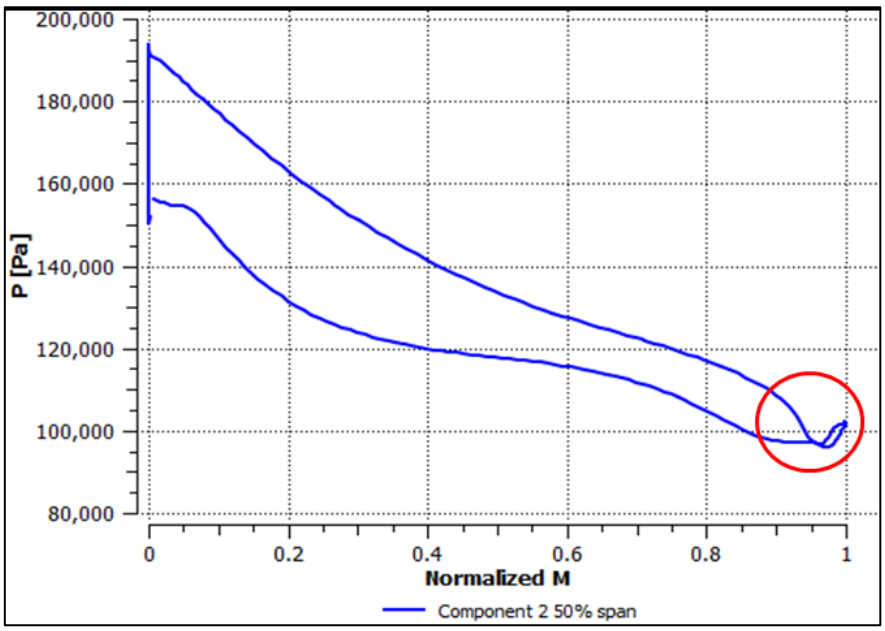

Figure 17: Rotor wheel blades loading chart

3.3 STRUCTURAL ANALYSIS RESULTS:

A Finite Element Analysis was conducted in order to assess the stress distribution for the turbine wheel. The FEA was performed using ANSYS Workbench. A static structural analysis was carried out. This is necessary because of the high rotational speed and high flow temperature experienced by the impeller. The alloy Inconel 718 was selected because of its high-quality mechanical properties under extreme temperatures. To ensure safe behaviour under working conditions, the Von Mises yield criterion needs to be satisfied. This criterion states that a material is said to start yielding when its Von Mises stress reaches a critical value known as the Yield strength. The Yield strength is defined as the stress at which a material begins to deform plastically. Inconel 718 0.2% Yield strength for different temperatures is presented in table 7.

Table 7: Inconel 718 0.2% Yield strength.

Temperature (°C)	0.2% Yield strength (MPa)
93	1172
204	1124
316	1096
427	1076
538	1069
649	1027
760	758

An iterative process modifying the turbine geometry was followed with the main aim to reduce Von Mises stress below 540 MPa on it. The reason is to obtain sufficient margin of error considering a safety factor of 1.4 respecting the Yield strength of the rotor material at 760°C which is over the maximum temperature (730°C) on the tip of the blades. To achieve this goal several attempts were made to obtain the stress results lower than the required stress limit. The main ways to achieve this objective are to scallop the back face of the rotor and introducing fillets on the roots of the blades and the at the shaft root at the back face of the turbine as shown in figure 18 and 19, also, material has been removed from the turbine back face as appears in figure 19 (the red line shows the back face profile before cutting material).

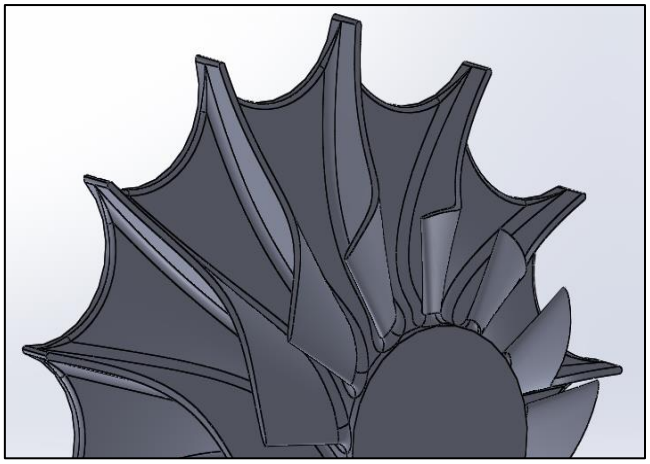

Figure 18: Rotor geometry after scalloping and introducing the fillet to roots of the blades.

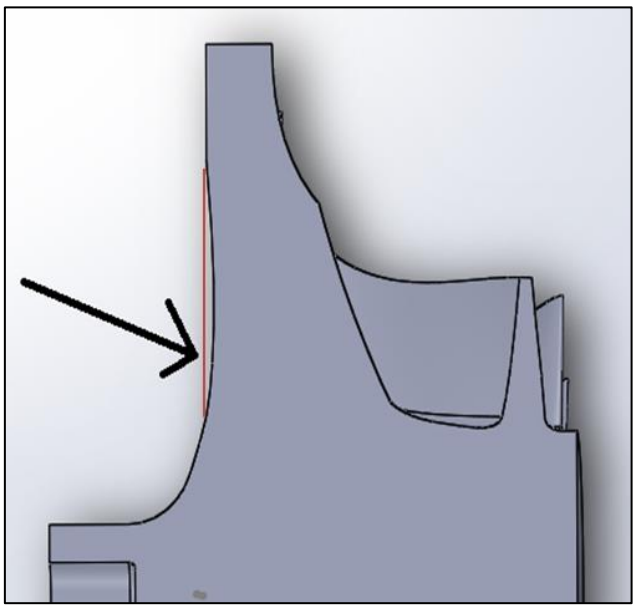

Figure 19: A section of the rotor showing the material removal from its back face.

The mesh used in the FEA contains 2284103 nodes and 1534875 elements. A view of the mesh is shown in figure 20. A rotational speed of 140000 rpm was used instead of 130000 rpm, which is the design point speed, as a safety practice for an off-design case. Also, a cylindrical support fixing radial, tangential and axial movements in the threaded hole

attached to the shaft was applied to simulate real conditions. To account for thermal expansion, a constant thermal load of 730°C was applied.

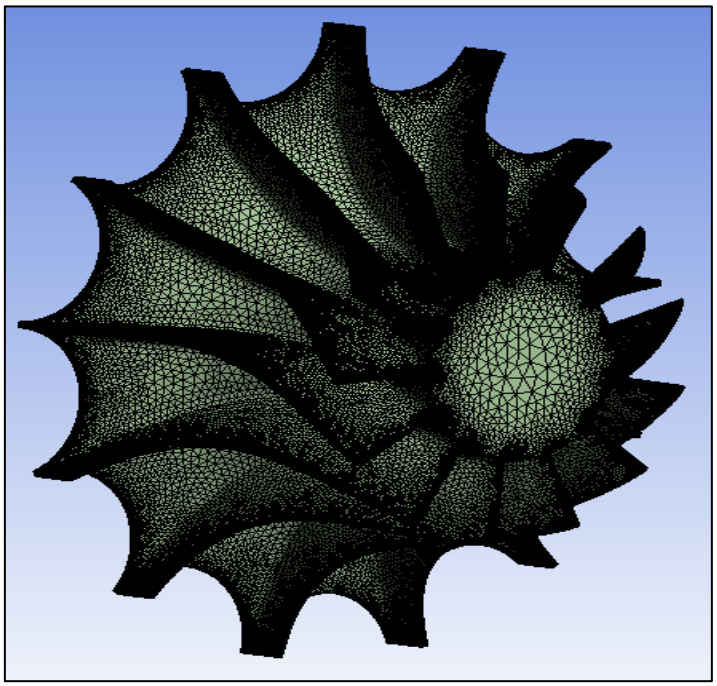

Figure 20: Structural mesh for the turbine rotor.

The FEA have been performed on the turbine rotor to check the structural integrity and the total deformation due to the thermal load. Figures 21, 22 and 23 show the stress distribution on the blades, back face and inside the turbine rotor. The maximum stress value is 522.6 MPa and it occurs in the back face of the rotor which is lower than the 540 MPa required for the intended factor of safety 1.4.

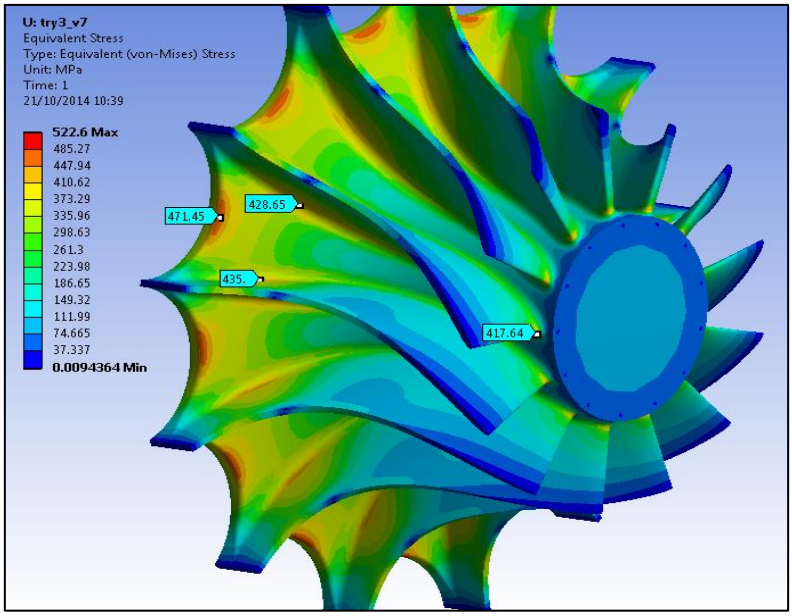

Figure 21: Von-Mises stress distribution along the rotor blades

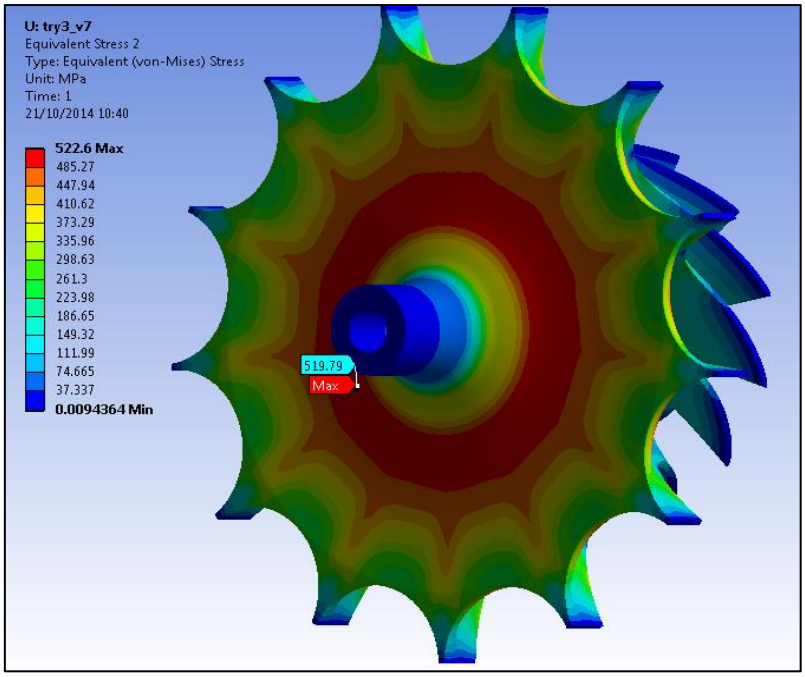

Figure 22: Von-Mises stress distribution on the rotor backface.

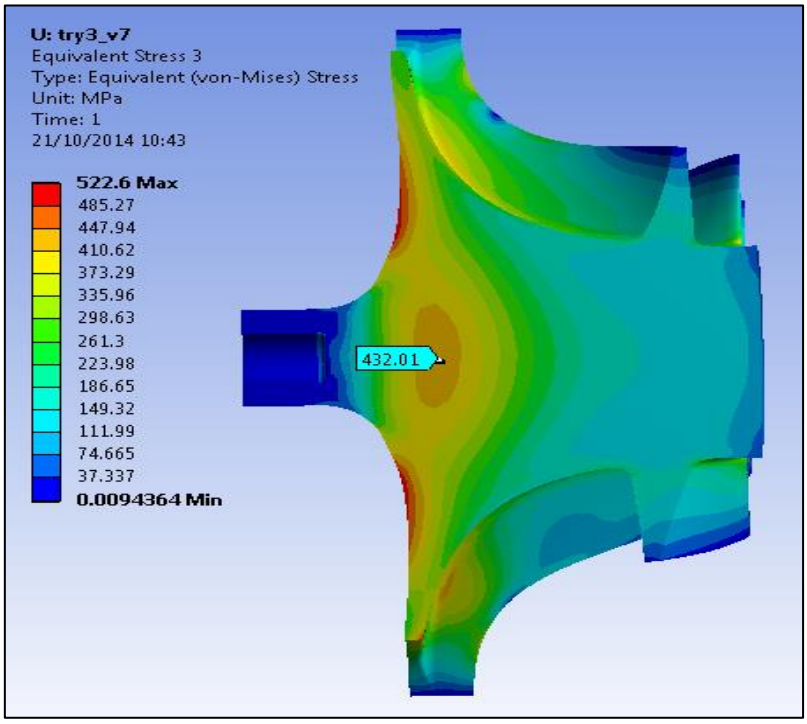

Figure 23: Von-Mises stress distribution inside the rotor.

Figure 24 shows the thermal expansion of the rotor blades. The maximum expansion is 0.07 mm occurring at the rotor's inlet which equivalent to about ~2% of the span length.

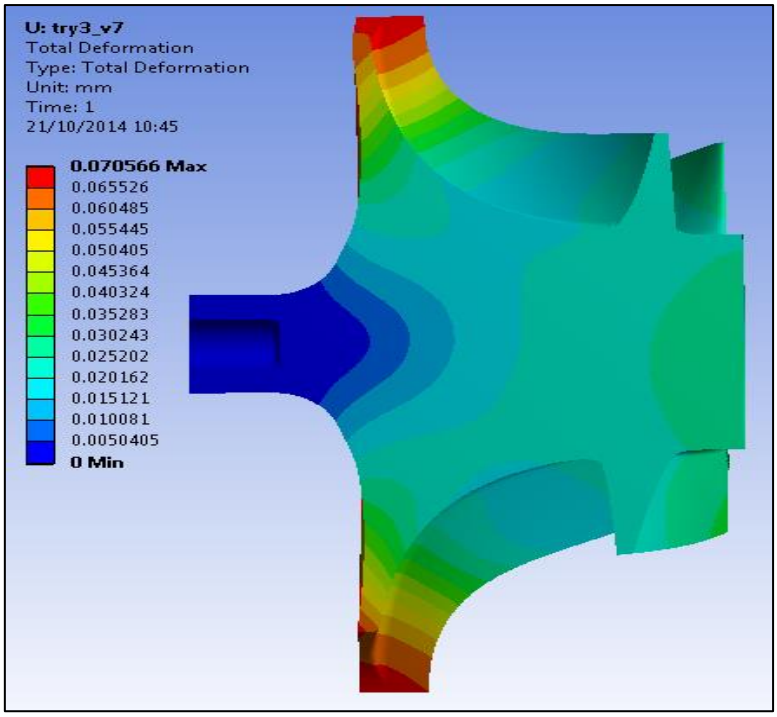

Figure 24: blades expansion due to the thermal load from the inlet gas.

4- CONCLUSIONS:

A turbine for a 5 kWe microgas turbine has been designed with efficiency of 83.3 % at the design point. The turbine was designed to meet the CSP system requirements. The design method developed in this work takes into account further development in CSP system, so the turbine structure was tested to operate at 900 °C, which is the state of the art turbine inlet temperature. Increasing the turbine inlet temperature, results in higher cycle efficiency for gas turbine. Also the turbine was tested to operate at higher rotational speed (140 krpm) than the design speed for safety.

To reduce the stresses on the turbine wheel, shallow scalloping has been done, meanwhile to reduce the inertia of the wheel and the stresses, material have been removed from the back face as discussed in section 3.3. The reason behind this is to reduce the aerodynamic loss due scalloping, as the deep scalloping could reduce the turbine efficiency by 4%.

ACKNOWLEDGMENT:

The author would like to acknowledge the contributions of Mr Mohsen Ghavami for performing the cycle analysis calculations for the gas turbine, and Mr Antonio Arroyo for performing the FEA for the designed turbine.

REFERENCES:

1- A Whitefield and N C Baines, "*Design of Radial Turbomachines*", Longman Scientific and Technical, 1990.

2- C Rodgers, "5-25 KWe Micro-Gas turbines Design Aspects", Proceeding of ASME TURBOEXPO 2000,May 8-11, 2000, Munich Germany.

3- C Rodgers. "Microturbine Rotational Speed Selection." Proceeding ASME TURBOEXPO 2013,

4- H Mustapha, Mark Zelesky, David Japikse and N C Baines, "*Axial and Radial Turbines*", Concepts NREC USA 2003.

5- G F Heitt and I H Johnston, "Experiments concerning the aerodynamic performance of inward flow radial turbines", Proc. IMechE 1964, Vol. 178, Pt 3I(ii), pp. 28-42.

6- I Watanabe, I Ariga and T Mashimo 1971, "Effect of dimensional parameters of impellers on performance characteristics of a radial-inflow turbine", *Trans. ASME, Journal of Engineering for Power*. pp. 81-102

7- M J Atkinson, "Design of Efficient Radial Turbines for Low Power Applications", PhD Theses, April 1998 University of Sussex.

8- P A Jacob, Carlos Ventura, Andrew S Rowlands and Emilie Sauret. "Preliminary design and performance estimation of radial inflow turbines: an automated approach". *Trans. ASME, Journal of Fluids Engineering*. Volume 134. 2012

9- R H Aungier, "*Turbine aerodynamics: axial-flow and radial-inflow turbine design and analysis*". ASME press, New York, 2006.

10- OE Balje. *Turbomachines: A Guide to Design, Selection, and Theory, 1981*. 1st ed. USA: John Wiley.

APPENDIX:

Table 8 contains the parameters needed to construct the volute geometry. As the volute was designed to be axisymmetric with circular cross section, then the data needed to construct it is: the radius of each cross section around the volute axis and the coordinates of the circle center of that section.

Table 8: Volute design data.

Volute Angle (°)	0.0	30.0	60.0	90.0	120.0	150.0	180.0	210.0	240.0	270.0	300.0	330.0	360.0
Cross section radius (mm)	24.1	22.9	21.5	20.2	18.8	17.3	15.8	14.2	12.4	10.5	8.4	5.7	0.0
Circle X-cordinate (mm)	0.0	0.0	0.0	0.0	0.0	0.0	0.0	0.0	0.0	0.0	0.0	0.0	0.0
Circle Y-cordinate (mm)	83.4	70.7	39.9	0.0	-37.8	-63.7	-71.3	-59.7	-33.2	0.0	30.3	49.1	48.3
Circle Z-cordinate (mm)	0.0	40.8	69.0	77.7	65.5	36.8	0.0	-34.5	-57.5	-63.7	-52.4	-28.3	0.0